

## PLATELETS AND THROMBOPOIESIS

## Expansion of the neonatal platelet mass is achieved via an extension of platelet lifespan

Zhi-Jian Liu,<sup>1</sup> Karin M. Hoffmeister,<sup>2</sup> Zhongbo Hu,<sup>3</sup> Donald E. Mager,<sup>4</sup> Sihem Ait-Oudhia,<sup>4</sup> Marlyse A. Debrincat,<sup>5</sup> Irina Pleines,<sup>5</sup> Emma C. Josefsson,<sup>5</sup> Benjamin T. Kile,<sup>5</sup> Joseph Italiano Jr,<sup>2,6</sup> Haley Ramsey,<sup>1</sup> Renata Grozovsky,<sup>2</sup> Peter Veng-Pedersen,<sup>7</sup> Chaitanya Chavda,<sup>1</sup> and Martha Sola-Visner<sup>1</sup>

<sup>1</sup>Division of Newborn Medicine, Boston Children's Hospital, Boston, MA; <sup>2</sup>Division of Translational Medicine, Brigham and Women's Hospital, Boston, MA; <sup>3</sup>Division of Neonatology, University of Florida, Gainesville, FL; <sup>4</sup>Department of Pharmaceutical Sciences, University at Buffalo, State University of New York, Buffalo, NY; <sup>5</sup>Cancer and Hematology Division, The Walter and Eliza Hall Institute of Medical Research, and the Department of Medical Biology, University of Melbourne, Parkville, Australia; <sup>6</sup>Division of Hematology, Brigham and Women's Hospital and the Vascular Biology Program, Boston Children's Hospital, Boston, MA; and <sup>7</sup>College of Pharmacy, University of Iowa, Iowa City, IA

## Key Points

- Rapid growth and rising platelet counts result in a significant expansion of platelet mass during neonatal life.
- The rise in platelet counts is mediated by a prolongation in the neonatal platelet lifespan.

The fetal/neonatal hematopoietic system must generate enough blood cells to meet the demands of rapid growth. This unique challenge might underlie the high incidence of thrombocytopenia among preterm neonates. In this study, neonatal platelet production and turnover were investigated in newborn mice. Based on a combination of blood volume expansion and increasing platelet counts, the platelet mass increased sevenfold during the first 2 weeks of murine life, a time during which thrombopoiesis shifted from liver to bone marrow. Studies applying *in vivo* biotinylation and mathematical modeling showed that newborn and adult mice had similar platelet production rates, but neonatal platelets survived 1 day longer in circulation. This prolonged lifespan fully accounted for the rise in platelet counts observed during the second week of murine postnatal life. A study of pro-apoptotic and anti-apoptotic Bcl-2 family proteins showed that neonatal platelets had higher levels of the anti-apoptotic protein Bcl-2 and were more resistant to apoptosis induced by the Bcl-2/Bcl-xL inhibitor ABT-737 than adult platelets. However, genetic ablation or pharmacologic inhibition of Bcl-2 alone did not shorten neonatal platelet survival or reduce platelet counts in newborn mice, indicating the existence of redundant or alternative mechanisms mediating the prolonged lifespan of neonatal platelets. (*Blood*. 2014;123(22):3381-3389)

## Introduction

Thrombocytopenia affects 18% to 35% of infants admitted to the Neonatal Intensive Care Unit (NICU).<sup>1,2</sup> The incidence of thrombocytopenia is inversely proportional to the gestational age, reaching 70% among the most preterm of infants.<sup>3</sup> The reasons underlying the predisposition of neonates to develop thrombocytopenia are unclear, but are likely related to the unique characteristics of fetal/neonatal megakaryocytes (MKs), which are regulated by a developmental stage-specific interplay of pathways, transcription factors, and microRNAs.<sup>4-6</sup> Although the molecular mechanisms accounting for the differences between fetal/neonatal and adult MKs are becoming increasingly clear,<sup>7</sup> our understanding of thrombopoiesis and platelet homeostasis during fetal/neonatal life has lagged behind.

Platelets have a finite lifespan in the circulation, normally 7 to 10 days in humans and 3 to 5 days in mice. Studies have shown this lifespan to be underpinned by a Bcl-2 family-mediated program that initiates the apoptotic death and subsequent clearance of aged platelets from the bloodstream.<sup>8,9</sup> The Bcl-2 family includes the prosurvival proteins Bcl-2, Bcl-x<sub>L</sub> and Mcl-1, the pro-apoptotic members Bak and Bax, and the BH3-only proteins. The latter promote apoptosis in

nucleated cells by directly activating Bak and Bax, and/or by inactivating the prosurvival family members.<sup>10,11</sup> In platelets, the critical prosurvival protein is Bcl-x<sub>L</sub>, which functions to restrain the activity of Bak and Bax.<sup>8</sup> Genetic deletion or pharmacological inhibition of Bcl-x<sub>L</sub> triggers platelet death and causes thrombocytopenia in humans, dogs, and mice.<sup>8,9,12-14</sup> Deletion of prodeath Bak and Bax leads to an almost doubling of platelet lifespan.<sup>8,15</sup> In addition, it is known that senescent platelets are selectively removed in response to specific surface signals,<sup>16-18</sup> and novel factors have been suggested to play a role in determining platelet lifespan.<sup>19,20</sup> The mechanisms regulating adult platelet homeostasis have been and continue to be extensively studied. In contrast, little is known about platelet production and turnover in fetal/neonatal life, the time when humans as well as mice experience the fastest growth in their lifetimes.

This study was designed to answer these questions, which are critical to understanding basic neonatal physiology as well as the susceptibility of preterm neonates to develop thrombocytopenia. We used a newborn mouse model to characterize platelet production

Submitted June 12, 2013; accepted February 24, 2014. Prepublished online as *Blood* First Edition paper, March 5, 2014; DOI 10.1182/blood-2013-06-508200.

The online version of this article contains a data supplement.

There is an Inside *Blood* Commentary on this article in this issue.

The publication costs of this article were defrayed in part by page charge payment. Therefore, and solely to indicate this fact, this article is hereby marked "advertisement" in accordance with 18 USC section 1734.

© 2014 by The American Society of Hematology

and turnover during the transition from fetal to adult hematopoiesis during the first 2 weeks of murine postnatal life, a period characterized by a developmentally unique combination of rapid growth and rising platelet counts. Using *in vivo* biotinylation to perform platelet kinetic studies in combination with mathematical modeling, we found that the platelet production rate was similar in newborn and adult mice, but platelet lifespan was significantly longer in neonates. An investigation of apoptotic and anti-apoptotic proteins showed that neonatal platelets had higher levels of the anti-apoptotic protein Bcl-2, and were more resistant to apoptosis induced by the Bcl-2/Bcl-x<sub>L</sub> inhibitor ABT-737, than their adult counterparts. However, genetic ablation or pharmacologic inhibition of Bcl-2 alone did not shorten neonatal platelet survival or reduce platelet counts in newborn pups, indicating the existence of redundant or alternative mechanisms underlying the prolonged lifespan of neonatal platelets.

## Materials and methods

### Animals

C57BL/6-SV129J mice were housed in a pathogen-free environment. The Boston Children's Hospital Animal Care and Use Committee or the Walter and Eliza Hall Institute Animal Ethics Committee approved all animal experiments.

### Murine blood sampling

Blood was collected through retroorbital puncture in adult mice. In newborn mice, the superficial temporal or the anterior facial vein was punctured with a 30-gauge needle. Blood at the puncture site was collected with a micro-pipette calibrated to 2 or 5  $\mu$ L and immediately diluted. Mean platelet volume (MPV) was measured in a Sysmex XT-2000i automated hematology analyzer (Sysmex, Kobe, Japan).

### Human blood samples

Human blood samples were collected with IRB approval from healthy adult donors (peripheral blood [PB]) or term Caesarean section deliveries (umbilical cord blood [CB]). This study was conducted in accordance with the Declaration of Helsinki.

### Histology, immunohistochemistry, and immunofluorescence

Murine liver, spleen, and bone marrow (BM) samples were fixed in 4% paraformaldehyde, embedded in paraffin, and sectioned. Bone samples from P10, P14, and adult mice were decalcified with 300 mM EDTA. For histologic analysis, sections were stained with hematoxylin and eosin (H&E).

Following antigen retrieval and blocking, MKs were immunohistochemically stained with a rabbit anti-von Willebrand Factor (VWF) antibody (DAKO, Denmark), as described.<sup>21</sup> At least 50 MKs were analyzed in each sample.

For immunofluorescence, after antigen retrieval and blocking, sections were incubated with rabbit anti-human PF4 (PreproTech, Rocky Hill, NJ), followed by an Alexa-593-conjugated anti-rabbit secondary antibody. After blocking again, sections were sequentially incubated with anti-VWF, Alexa-488-conjugated secondary antibody, and DAPI. Images were analyzed in a Nikon Eclipse fluorescent microscope equipped with a Nikon DXM1200F camera.

### Flow cytometry of murine spleen MKs

Spleens were collected from P5-P10 and adult mice. After mincing, tissue was passed through 16G and 18G needles (5 times each) and through a 100-micron cell strainer. Dissociated cells were washed twice and incubated with a PE-conjugated anti-mouse CD41 (MWreg30; BD Biosciences, San Jose, CA). MKs were then enriched using a magnetic PE selection kit (Stemcells, Vancouver, Canada), incubated with Hoechst 33342 (Sigma-Aldrich,

St. Louis, MO), and stained with APC-conjugated anti-mouse CD61 (Invitrogen, Grand Island, NY). The ploidy of CD41<sup>+</sup>/CD61<sup>+</sup> MKs was analyzed in an LSR Fortessa Cell Analyzer (BD Biosciences).

### Ultrastructure of flow-sorted MKs

MKs were separated and enriched as described earlier. 2-4N MKs were flow-sorted and processed for EM as previously described.<sup>22</sup>

### Platelet counts

Platelet counts were determined by flow cytometry using a modified published method.<sup>23</sup> Diluted samples were labeled with PE-conjugated anti-mouse CD41, and were mixed with a known number of FITC-labeled SPHERO beads (Spherotech, Libertyville, IL). The number of CD41-positive platelets was measured by flow cytometry when the bead count reached 2000.

### Blood volume determination

Washed RBCs were biotinylated with sulfo-NHS-biotin (Pierce Chemical, Rockford, IL) and transfused into newborn (through the superficial temporal vein)<sup>24</sup> or adult mice. Blood was drawn 30 minutes after transfusion, and the blood volume was calculated as described.<sup>25</sup>

### Platelet survival

*In vivo* platelet biotinylation was performed as previously described.<sup>26</sup> NHS-biotin solution (10 mg/mL for adult mice and 5 mg/mL for newborn mice) was infused intravenously at a dose of 10  $\mu$ L per gram body weight. Starting 1 hour postinfusion, blood (2  $\mu$ L) was collected every 24 h. Diluted blood samples were incubated with FITC-Avidin and PE-conjugated anti-mouse CD41, and the percentage of biotinylated platelets was determined by flow cytometry. The total number of biotinylated platelets was calculated at each time point by multiplying platelet count  $\times$  biotinylated platelet percentage  $\times$  blood volume. Data were expressed as percent change in total biotinylated platelets from the 24-hour time point.

To study transfused platelets, platelets from adult mice were washed and labeled with 5-chloromethylfluorescein diacetate (CMFDA, Invitrogen) as described.<sup>17</sup> P3 mice were transfused with 20  $\mu$ L, and adult mice with 10  $\mu$ L/g of the same platelet suspension ( $5 \times 10^8$  platelets/mL). At 2 minutes and 2, 6, 24, 48, and 72 hours posttransfusion, 2  $\mu$ L of blood were collected, diluted, and labeled with CD41. The percentage of CMTFA-labeled platelets was determined by flow cytometry, and the total number of labeled platelets at each point was calculated as described for biotinylated platelets. Data were expressed as percent change in total labeled platelets.

### In vitro platelet survival

Platelet-rich plasma (PRP) was prepared from CB and PB and was incubated at 37°C in 5% CO<sub>2</sub> for 5 days.<sup>27</sup> Every 24 hours, a PRP aliquot was incubated with 500 nM prostaglandin E1 (PGE1), and labeled with an APC-conjugated anti-CD41 (BD Pharmingen, San Diego, CA). After incubating with a 400 nM JC-1 solution, live platelets were identified based on the distribution in the PE- and FITC-channels. Separate aliquots were incubated with Annexin V-PE (BD Pharmingen) and FITC-conjugated anti-human P-selectin, and they were analyzed by flow cytometry.

To determine the effects of ABT-737 and ABT-199, freshly isolated PRP was treated with PGE1. Platelets were washed twice and were resuspended to a density of  $1 \times 10^8$ /mL. Aliquots of this platelet suspension were incubated for 2 hours at 37°C with ABT-737 or ABT-199 at final concentrations of 10 to 10 000 nM.<sup>28</sup> Platelets were labeled with PE-conjugated anti-human CD41 and APC-annexin V and were analyzed by flow cytometry.

### Platelet protein analysis

PRP was prepared from CB and PB. After a second centrifugation, platelets were incubated with PGE1, resuspended in PBS+EDTA, and incubated with PE-conjugated mouse anti-human CD45 and anti-glycophorin antibodies (BD Pharmingen). Residual red and white cells were removed by magnetic separation using a PE selection kit (Stemcell Technologies, Canada). Platelets were then washed and lysed in RIPA buffer (Sigma-Aldrich). Western blot

was performed using anti-human Bcl-2, Bcl-x<sub>L</sub>, Bax, Bak, Caspase-3, Caspase-9, Mcl-1, Bad, Bid, Bik, Bim, PUMA (all Cell Signaling, Danvers, MA), GAPDH (Santa Cruz Biotech, CA) and  $\beta$ -actin (Rockland, MA) antibodies. ImageJ 1.45 software was used for quantification.

Bcl-2 and Bcl-x<sub>L</sub> in mouse platelets were evaluated by intracellular flow cytometry. Diluted blood was incubated with PE-conjugated anti-mouse CD41 (BD Pharmingen) for 15 minutes, fixed with 0.8% PFA, and permeabilized with prechilled methanol on ice for 30 minutes. After washing, platelets were stained with FITC-conjugated anti-Bcl-x<sub>L</sub> (Cell Signaling) and Alexa 647-conjugated anti Bcl-2 (BioLegend, San Diego, CA).

### Statistical analysis

Two-way analysis of variance was used for multiple comparisons and Student *t* test for pairwise comparisons. All analyses were performed using GraphPad Prism (version 4) software.

## Results

### Transition from fetal to adult megakaryopoiesis

The transition from fetal to adult megakaryopoiesis was analyzed in C57BL/6 mice. First, we evaluated H&E sections of liver, spleen, and BM obtained from postnatal day 1 (P1), P3, P5, P7, P10, P14, and adult (8 weeks old) mice. As shown in Figure 1, the liver of P1 and P3 mice contained abundant hematopoietic islands among disorganized hepatocytes. Starting at P5, hematopoietic islands became increasingly rare and hepatocytes began to organize. In contrast to liver, the BM of P1 and P3 mice was markedly hypocellular. BM cellularity started to increase at P5, and reached nearly 100% by P14.

Next, MKs were stained with anti-VWF, and the MK size and concentration were evaluated in liver, spleen, and BM samples at the same time points. Matching the histologic observations, the liver MK concentration decreased sharply between P3 and P7. In contrast, the BM MK concentration increased during the first 2 weeks of life, and by P14 it was only slightly lower than in the adult BM. The MK concentration in the spleen increased approximately sixfold in the first 10 days of life, and then decreased back to basal levels in adult mice (Figure 2A). During this transition, the MK size increased steadily in all 3 organs, and it reached values only slightly lower than the adults by P14 (Figure 2B). Taken together, these observations suggested that the transition from fetal to adult megakaryopoiesis is nearly completed in the first 2 weeks of life in C57BL/6 mice, and that the spleen supports thrombopoiesis during this period.

Because splenic MKs from P5 to P7 were significantly smaller than those in adult mice, we then asked whether they were mature and similar to human neonatal MKs.<sup>22</sup> To assess this, we evaluated for the presence of PF4 and VWF, both found in  $\alpha$  granules of mature MKs. As shown in Figure 2C, typical MKs in the adult BM were large, with a multilobular nucleus and a granular PF4/VWF double-positive cytoplasmic staining pattern that was consistent with  $\alpha$ -granules. P7 splenic MKs were small in comparison and had a single nucleus, but they were also strongly double-positive for PF4 and VWF, suggesting that they were mature.

To evaluate further these small neonatal MKs, CD41-positive cells were enriched from the spleen of P5-P10 and adult mice and were analyzed by flow cytometry and EM. A total of 95% of newborn splenic MKs had a ploidy of 2-4N, compared with 51.6% of adult MKs (Figure 2D). When examined by EM, ~30% of 2-4N neonatal MKs exhibited an open invagination membrane system (Figure 2E and supplemental Figure 1), characteristic of mature MKs (see supplemental Data available at the *Blood* Web site).

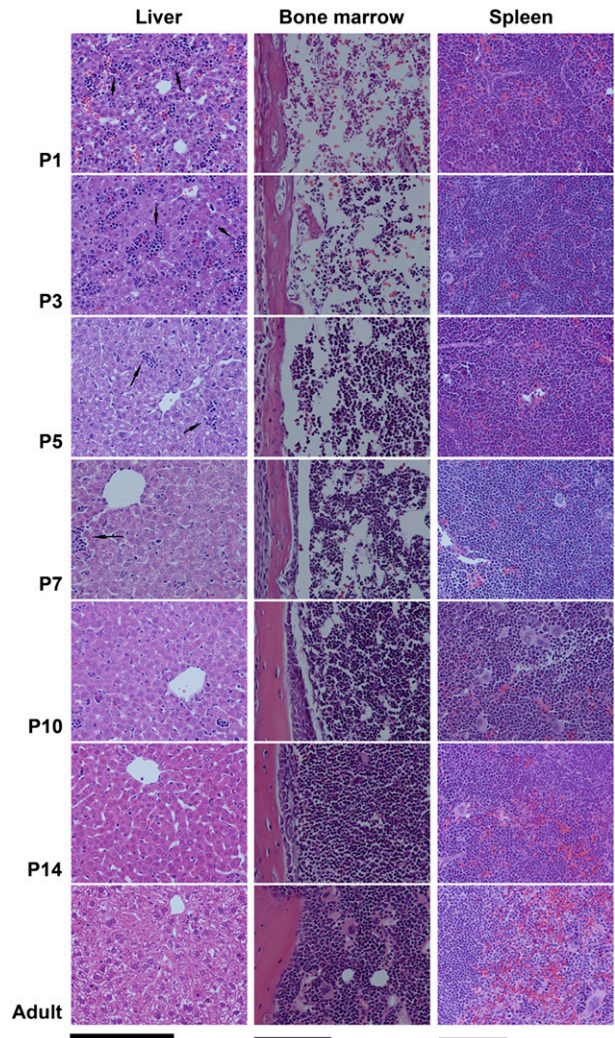


**Figure 1. Transition from fetal to adult murine hematopoiesis.** Histologic changes in the liver, spleen, and BM of newborn mice during the first 2 weeks of life, compared with adults. Fixed tissue sections were stained with H&E and photographed with a  $\times 20$  objective lens (Bar: 50  $\mu$ m). (Left column) The liver of P1 and P3 newborn mice contained numerous hematopoietic islands (arrows), which rapidly decreased after P5. (Middle column) The BM of newborn pups during the first week of life was markedly hypocellular, containing large sinusoids and limited hematopoietic elements. (Right column) Clearly distinct red and white pulp zones were formed in the spleen and increased in size during the first 2 weeks of life.

### Blood volume and platelet counts during neonatal development

We hypothesized that the rapid increase in body weight during early postnatal life would be correlated with rapid blood volume expansion. As shown in Figure 3A, healthy newborn mice increased their weight rapidly, from  $1.3 \pm 0.1$  gram at P1 ( $n = 42$ ) to  $7.3 \pm 0.7$  gram at P14 ( $n = 16$ ). To test whether the ratio of blood volume to body weight was stable or changed with age, we measured the blood volume in P3, P6, and adult mice.<sup>25</sup> These studies showed a strong correlation between body weight and blood volume ( $R^2 = 0.992$ ; Figure 3B), with a blood volume of  $\sim 70.5 \mu\text{L/g}$  at all postnatal ages (95% confidence interval 66.8-74.3  $\mu\text{L/g}$ ). Overall, blood volume increased 5.5-fold during the first 2 weeks of murine life.

Platelet counts during the same period were determined by flow cytometry.<sup>23</sup> At P1, the mean platelet count was  $596 \pm 139 \times 10^3/\mu\text{L}$  ( $n = 11$ ), which was approximately half of the adult count. These values remained relatively stable during the first week, but they nearly doubled between P7 and P10 (Figure 3C). By P14, the platelet

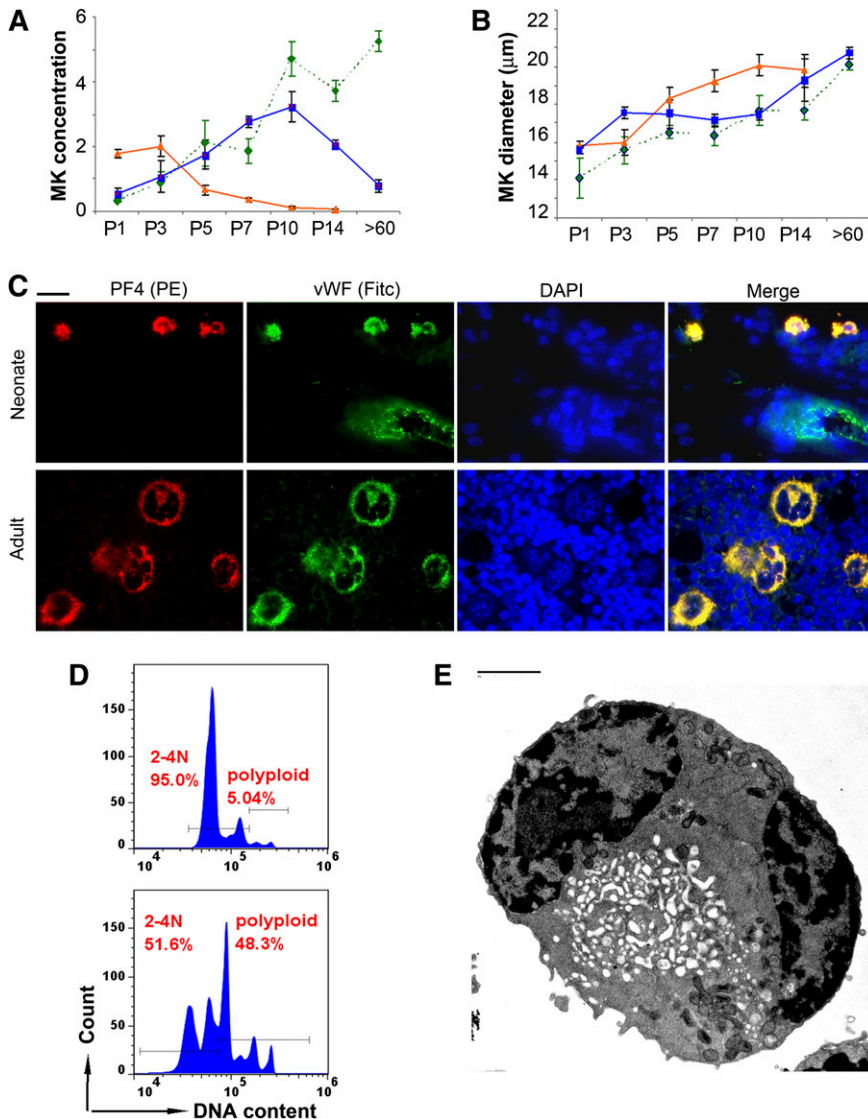


**Figure 2. Megakaryopoiesis during murine neonatal development.** MK concentration (A) and MK diameter (B) were measured in the liver (orange triangles and solid line), BM (green diamonds and interrupted line), and spleen (blue squares and solid line) of newborn mice on days P1, P3, P5, P7, P10, and P14, and in adult mice (>60 days) after immunohistochemical staining with anti-VWF. Data presented are means  $\pm$  SD from at least 4 mice at each time point. (A) MK concentration, expressed as number of MKs present in an area of tissue measuring  $250 \times 250 \mu\text{m}$  at  $\times 400$ . (B) MK diameter (in  $\mu\text{m}$ ) measured under the microscope at  $\times 400$ . (C) MK maturation was analyzed by immunofluorescent staining for VWF (green) and PF4 (red). Shown are representative neonatal MKs (spleen, upper row) and adult MKs (BM, lower row). Note a blood vessel in the upper panel, with visible endothelial cells expressing only VWF (green). All photomicrographs were obtained at  $\times 400$ . Bar:  $10 \mu\text{m}$ . (D) MKs isolated from the spleen of newborn mice (P5-P10, top) were compared with MKs from the spleen of adult mice (bottom). The ploidy of CD41/CD61 double-positive cells was determined by flow cytometry after staining with Hoechst 33342. (E) Ultrastructure was analyzed by electron microscopy in flow-sorted 2-4N MKs isolated from the spleen of neonatal mice (P5-P10). Despite their small size,  $\sim 30\%$  of 2-4N neonatal MKs were mature, as indicated by the presence of an open demarcation membrane system. (Bar:  $2 \mu\text{m}$ )

count was close, but was still significantly lower, than the count in adult mice ( $1140 \pm 175$  vs  $1362 \pm 146 \times 10^3/\mu\text{L}$ , respectively;  $P < .05$ ).

To estimate the total number of platelets per animal, we multiplied the platelet count by the blood volume. P1 mice had an average of  $55 \pm 14 \times 10^6$  platelets ( $n = 11$ , Figure 3D). During the first 2 weeks of life, the total platelet number per animal increased nearly 11-fold, up to  $581 \pm 91 \times 10^6$  by P14 ( $n = 15$ ). During that same period, the MPV decreased from  $8.6 \pm 0.3$  fL in P1 mice to  $6.2 \pm 0.1$  fL by P14 (Figure 3E). The total platelet mass, calculated by multiplying the total platelet number by the MPV, expanded sevenfold, from  $0.47 \pm 0.1 \mu\text{L}$  in P1 mice ( $n = 11$ ) to  $3.51 \pm 0.5 \mu\text{L}$  in P14 animals ( $n = 15$ ) (Figure 3F).

#### Platelet production and turnover during neonatal development

To evaluate platelet production and turnover in newborn and adult mice, we then measured platelet lifespan using *in vivo* biotinylation. Following intravenous injection of a single dose of NHS-biotin into P1 ( $n = 16$ ) and adult mice ( $n = 7$ ), the total number of biotinylated platelets was calculated every 24 hours by multiplying platelet count, blood volume, and biotinylated platelet percentage. The total number of biotinylated platelets 24 hours postinjection was considered

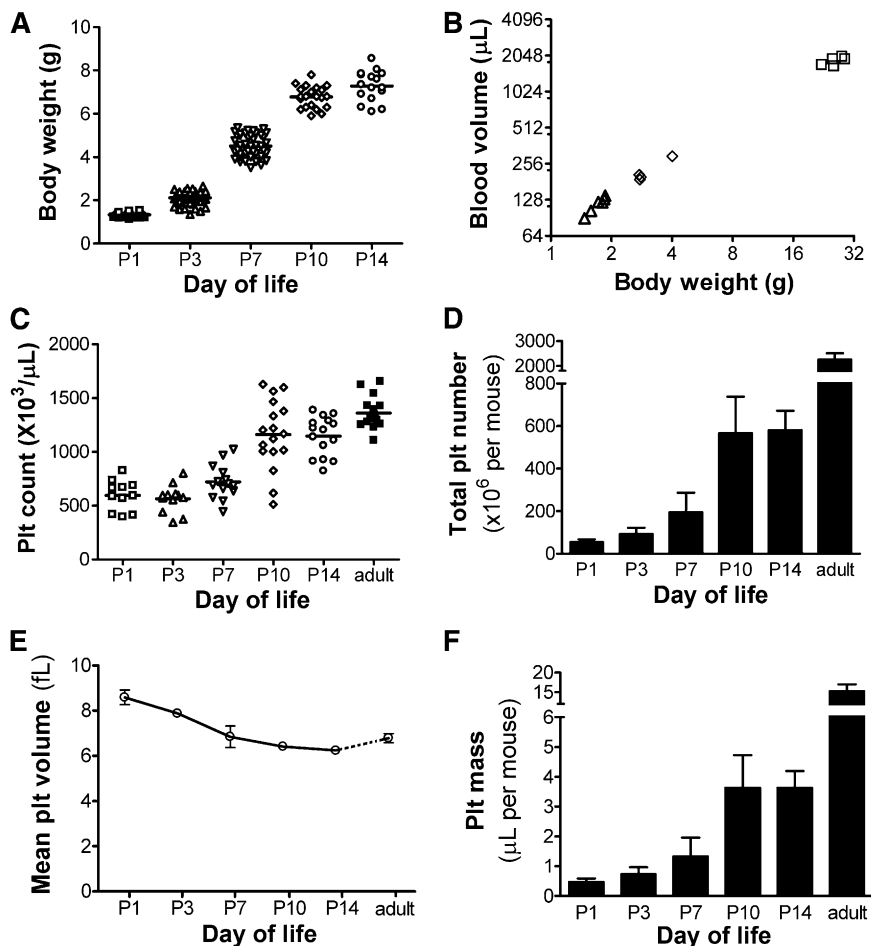
100%, and percent changes were followed from that point (Figure 4A). These studies indicated that neonatal platelets had a significantly longer lifespan than adult platelets.

Serial data on platelet counts, biotinylated platelet percentages, and blood volume from 16 newborn and 7 adult mice were then incorporated into a mathematical time-dependent transduction model to describe the temporal profiles of labeled and total (labeled + non-labeled) platelets (supplemental Methods and supplemental Figure 2). In this model, the calculated platelet production rate (platelets/ $\mu\text{L}/\text{h}$ ) was similar in neonates and adults (Figure 4B). The platelet lifespan, however, was 25% longer in newborn compared with adult mice ( $4.9 \pm 1.3$  vs  $3.9 \pm 1.1$  days, respectively;  $P = .0083$ ). Based on model predictions, the lifespan of neonatal platelets decreased to adult values by P14 (Figure 4C).

To test whether the prolonged lifespan of neonatal platelets was a result of cell-intrinsic factors vs developmental differences in platelet clearance, adult and P3 mice were transfused in parallel with CMFDA-labeled platelets isolated from adult mice. The kinetics of disappearance of these transfused platelets (Figure 4D) were different than those of endogenous, *in vivo* biotinylated platelets (Figure 4A), mostly because of a rapid decrease in the transfused platelets over the 6 hours following injection. Nevertheless, we found no differences

**Figure 3. Blood volume, platelet counts, and platelet mass during neonatal development.**

(A) Body weights were obtained in healthy mice during the first 2 weeks of life at the time points indicated. Each symbol represents an individual animal; horizontal lines indicate the mean for each group. (B) After transfusion with a known number of biotinylated RBCs, the blood volume was calculated in mice of different ages and was correlated to each animal's body weight. Each symbol represents an individual mouse. (C) Platelet counts were measured in the first 2 weeks of life and in adult mice at the ages indicated. Each symbol represents an individual animal; horizontal lines indicate the mean for each group. (D) Total platelet number was calculated for each animal by multiplying the platelet count  $\times$  blood volume (in  $\mu\text{L}$ ). The bars represent the mean  $\pm$  SD of at least 11 individual mice at each postnatal age indicated. (E) MPVs were measured in mice at the postnatal ages indicated. Each data point represents the mean  $\pm$  SD of 7 to 8 individual mice. (F) Total platelet mass was calculated in mice at the ages indicated by multiplying the platelet count  $\times$  the blood volume  $\times$  the MPV. Bars represent the mean  $\pm$  SD of at least 11 individual mice at each time point.



between neonates and adults in the survival of adult labeled platelets, suggesting that the differences in platelet lifespan were mostly cell intrinsic.

Next, we asked whether these findings were applicable to humans. To address this, given the ethical difficulties of conducting platelet survival studies in human neonates, we compared the survival of human neonatal (CB) vs adult (PB) platelets *in vitro*. Annexin V binding was used as a marker of apoptosis. Platelet activation was ruled out by confirming lack of P-selectin surface expression in the Annexin V-positive platelets (Figure 5A). As shown in Figure 5B, the percentage of Annexin V-positive platelets increased progressively during the incubation period. Starting on day 2, however, the percentage of apoptotic platelets was lower in CB-PRP compared with PB-PRP, with the most significant differences observed on day 3 ( $37.1 \pm 17.3\%$  in CB-PRP vs  $68.3 \pm 18.5\%$  in PB-PRP,  $n = 5$ ,  $P < .01$ ). Platelets on day 3 of incubation responded to PMA stimulation by increasing P-selectin expression, indicating that they were capable of degranulating (supplemental Figure 3).

In addition, the proportion of live platelets was determined using the fluorescent dye JC-1 for mitochondrial transmembrane potential. As shown in Figure 5C, the live platelet percentage was higher in CB-PRP compared with PB-PRP at all time points starting on day 2. The most significant differences were again observed on day 3, when  $23.9 \pm 15.9\%$  ( $n = 5$ ) of adult platelets remained alive, compared with  $63.9 \pm 7.5\%$  of CB platelets ( $n = 3$ ;  $P < .001$ ). During this period we observed a progressive decrease in the concentrations of Bcl-2 and Bcl-x<sub>L</sub>, and increases in the active forms of Caspase-9 and

Caspase-3, indicating activation of the intrinsic apoptosis pathway (supplemental Figure 4).

**Pro-apoptotic and anti-apoptotic Bcl-2 family proteins in neonatal vs adult platelets**

In recent years, several studies demonstrated that an important mechanism regulating platelet lifespan is the balance between anti-apoptotic and pro-apoptotic Bcl-2 family proteins.<sup>8</sup> Thus, we measured the protein concentrations of Bcl-2, Bcl-x<sub>L</sub>, Bak, Bax, Caspase-3, and Caspase-9 in freshly isolated human platelets purified from CB and PB ( $n = 8/\text{group}$ ). As shown in Figure 6A, we found no significant differences in the protein levels of Bcl-x<sub>L</sub>, Bak, Bax, Caspase-3, and Caspase-9. Bcl-2 concentrations, however, were nearly eightfold higher in CB compared with PB platelets (ratio to  $\beta$  actin:  $1.11 \pm 0.3$  vs  $0.14 \pm 0.1$ , respectively;  $P < .001$ ).

We then asked whether the same differences in Bcl-2 were present in murine platelets. Mirroring the human observations, we found higher Bcl-2 expression in platelets from newborn ( $n = 11$ ) compared with adult ( $n = 8$ ) mice ( $P < .05$ ), but no differences in Bcl-x<sub>L</sub> expression (Figure 6B).

**Effects of Bcl-2 inhibition on neonatal vs adult platelets**

Finally, we hypothesized that the high Bcl-2 protein levels would render neonatal platelets more resistant to apoptosis induced by Bcl-2 inhibitors. To test this, we first compared the effects of ABT-737, a BH3-mimetic that antagonizes Bcl-x<sub>L</sub> and Bcl-2, on purified neonatal and adult human platelets. Consistent with previous reports,

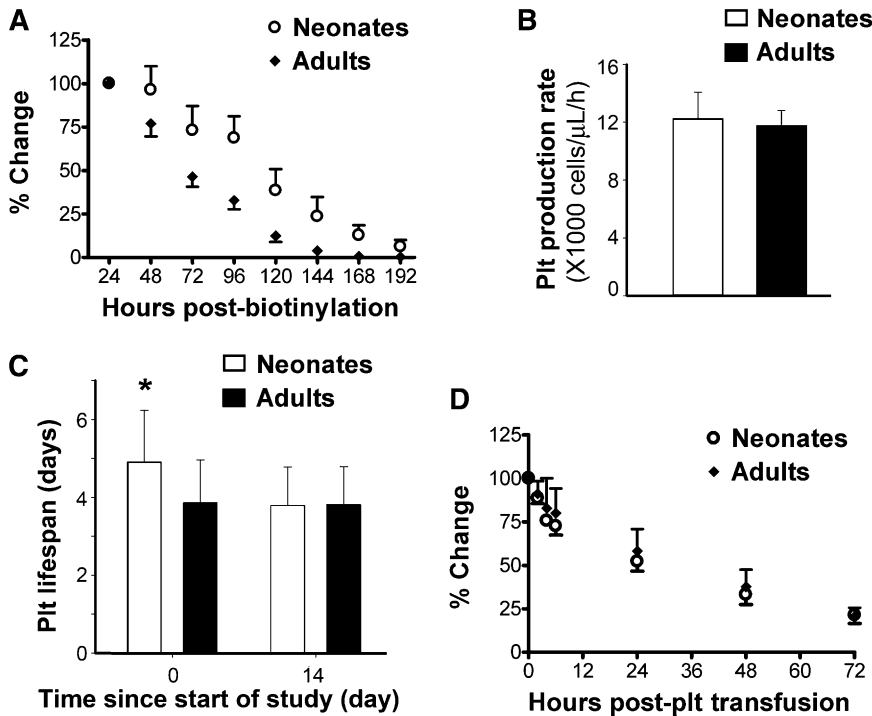


**Figure 4. Platelet production and survival in newborn vs adult mice.** (A) Platelet survival was compared between neonatal (n = 16) and adult (n = 7) mice using in vivo biotinylation. Changes in total biotinylated platelets were expressed as percent of the value 24 hours postbiotinylation. (B) A dynamic mathematical model was designed to compute platelet production rate, using data from the same 16 newborn and 7 adult mice. The results of the model indicated that the platelet production rate (expressed as number of platelets/μL of blood/h) was similar in newborn and adult mice. (C) The model also indicated that the platelet lifespan of newborn mice was significantly longer than that of adult mice ( $4.9 \pm 1.3$  vs  $3.9 \pm 1.1$  days; \* $P < .01$ ). The differences disappeared as newborn mice reached day 14 ( $3.8 \pm 1$  day). Details of the model are provided in the supplemental Methods and supplemental Figure 2. (D) Platelet turnover was further analyzed following transfusion of CMFDA-labeled adult platelets into newborn (n = 9) and adult (n = 12) mice. Changes in the number of transfused platelets were expressed as percent of that at 2 minutes posttransfusion.

incubation with ABT-737 for 2 hours induced platelet apoptosis in a dose-dependent manner.<sup>8,9,28</sup> Compared with adult platelets, neonatal platelets were less sensitive to ABT-737 at concentrations  $\geq 30$  nM ( $P < .05$ ), displaying a right-shift in the dose-response curve and a lower maximal effect (supplemental Figure 5A). To evaluate the effects of Bcl-2 inhibition alone, we then incubated human CB-derived platelets with escalating doses of ABT-199, a recently developed selective Bcl-2 inhibitor that does not antagonize Bcl-x<sub>L</sub>.<sup>29</sup> In contrast to the effects of the Bcl-2/Bcl-x<sub>L</sub> inhibitor

ABT-737, ABT-199 did not induce significant apoptosis of human neonatal platelets (supplemental Figure 5B).

Consistent with these in vitro observations, treatment of P3 mice with ABT-199 did not affect the platelet count or shorten the platelet survival in vivo (n = 8 per group; supplemental Figure 6A-B). Furthermore, we found no significant differences in platelet counts or reticulated platelet percentages between Bcl-2<sup>+/+</sup>, Bcl-2<sup>+/-</sup>, and Bcl-2<sup>-/-</sup> mice on P2, P5, P7, and P10 (supplemental Figure 6C-D).

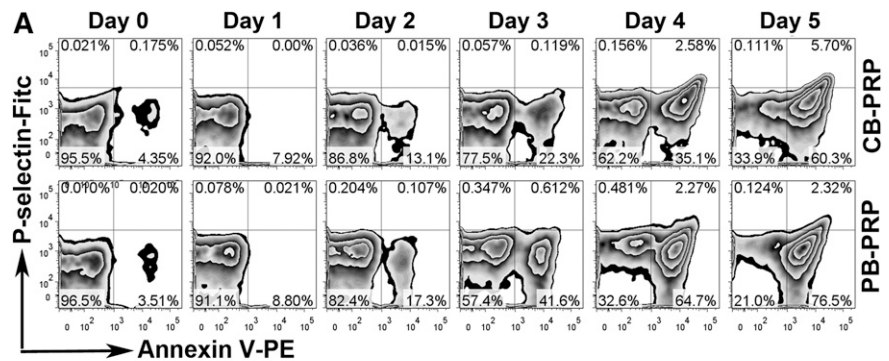


**Figure 5. Prolonged in vitro survival of human neonatal platelets.** In vitro survival of human neonatal and adult platelets was evaluated by incubating PRP from human umbilical CB and adult PB at 37°C for 5 days. (A) Annexin V-binding and P-selectin expression were evaluated daily by flow cytometry in CD41-gated CB and PB platelets during a 5-day incubation period. (B) Percentages of Annexin V positive platelets were quantified daily and compared between CB-PRP (n = 6) and PB-PRP (n = 8). (C) Platelet survival was quantified daily by FACS analysis after staining with the mitochondrial dye JC-1. The percentages of live platelets were measured in CB-PRP (n = 3) compared with PB-PRP (n = 5). \* $P < .05$ ; \*\* $P < .01$ ; \*\*\* $P < .001$ .

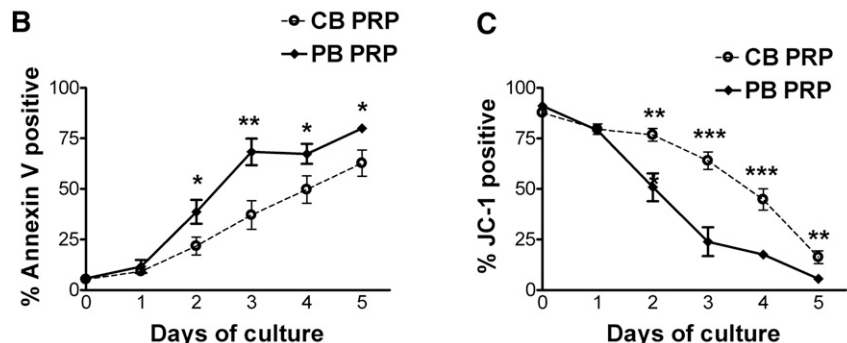
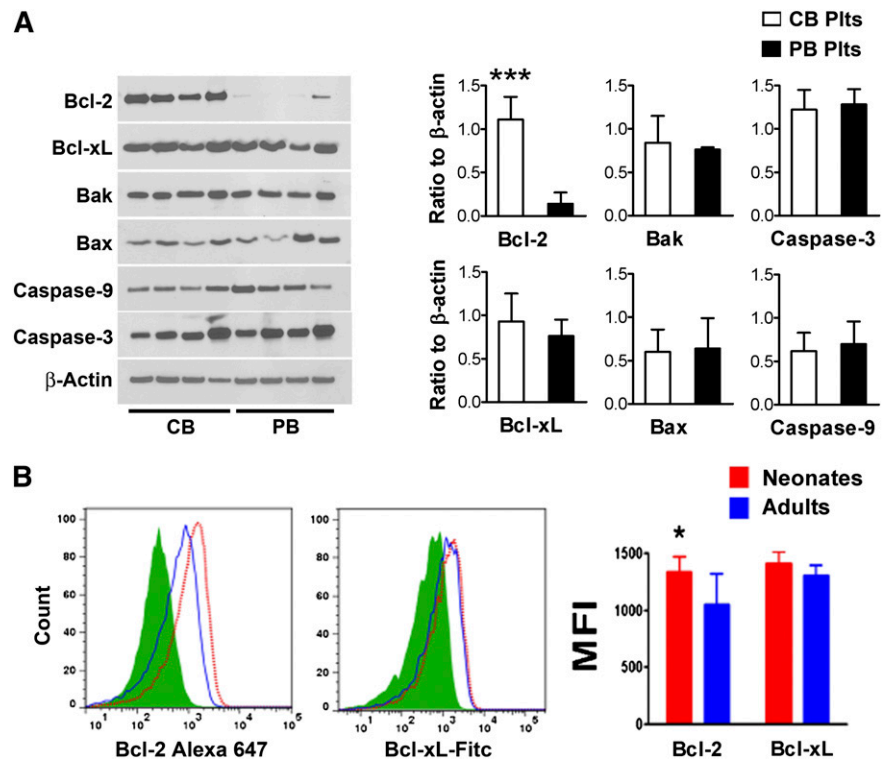


**Figure 6. Bcl-2 family proteins in neonatal vs adult platelets.** (A) Apoptosis-related proteins were quantified in freshly isolated purified human neonatal and adult platelets by western blot assay. The expression levels of Bcl-2, Bcl-x<sub>L</sub>, Bak, Bax, Caspase-9, and Caspase-3 are shown in representative western blots from 4 independent CB and 4 independent PB samples. The bars represent the mean  $\pm$  SD concentrations of these proteins in 8 independent CB (open bars) and 8 PB samples (filled bars), expressed as the ratio to  $\beta$  actin. \*\*\* $P < .001$ . (B) Expression levels of Bcl-2 and Bcl-x<sub>L</sub> were evaluated in neonatal and adult mouse platelets by flow cytometry. Representative histograms show Bcl-2 and Bcl-x<sub>L</sub> mean fluorescent intensity (MFI) levels in murine neonatal vs adult platelets. The bars represent the mean  $\pm$  SD MFI measurements from neonatal ( $n = 11$ ) and adult ( $n = 8$ ) murine platelets. \* $P < .05$ .



Because BH3-only proteins can also promote apoptosis, and deficiency of multiple BH3-only proteins leads to resistance to apoptosis in various cell types,<sup>10,30</sup> we then evaluated the protein concentrations of Mcl-1 and the BH3-only proteins Bad, Bid, Bik, Bim, and Puma in CB-derived and PB-derived human platelets ( $n = 4$ /group). As shown in supplemental Figure 7, we did not find significant differences between neonatal and adult platelets in any of the molecules evaluated.

## Discussion

To gain a better understanding of the susceptibility of neonates to develop thrombocytopenia, we used C57BL/6 newborn mice as a model to study thrombopoiesis during neonatal development. Consistent with earlier studies of hematopoiesis,<sup>31,32</sup> we found the fetal liver to be the major megakaryopoietic site at P1 and P3, followed by a sharp decrease after P5. The BM did not become the main megakaryopoietic organ until P10 to P14. During this transition, the spleen exhibited a sixfold increase in MK concentration, mimicking the splenic response to hematopoietic stress in adults. Unlike in adults, however (where the largest MKs are found in the spleen),<sup>33,34</sup> we found neonatal splenic MKs to be very small and of low ploidy but cytoplasmically mature, similar to cultured human neonatal MKs.<sup>22</sup> Although our findings suggest that the spleen contributes to thrombopoiesis during this period, the individual contribution of each organ to platelet production could not be quantified, because the size of the organ and the platelet yield per MK were unknown.

The first 2 weeks of postnatal murine life correspond developmentally to the last trimester of human pregnancy (24–40 weeks gestation), or to the period of time that extremely premature infants spend in the NICU. During that time, the human BM is well developed and human fetuses/preterm neonates finalize the transition from hepatic to marrow hematopoiesis, but the human spleen does not function as a hematopoietic organ.<sup>35</sup> Similar to newborn mice

during the first 2 weeks of postnatal life, human fetuses or neonates born at 24 weeks experience a fivefold increase in body weight throughout a 16-week period, during which their platelet count also increases.<sup>36</sup>

To evaluate the mechanisms through which neonates raise their platelet counts while their blood volume is rapidly expanding, we measured platelet survival in newborn mice and developed a mathematical model that was unique in that it took into account the complex dynamic changes occurring during this developmental period. This model indicated that neonates and adults have a similar platelet production rate (platelets/ $\mu$ L/h), but neonatal platelets survive 25% longer than adult platelets in the circulation. According to the model, this prolongation in platelet survival is transient and is no longer present by P14, and it fully accounts for the rise in platelet counts observed during the second week of murine life. The results of our in vitro human platelet survival studies strongly suggest that this long lifespan is also a feature of human neonatal platelets. Ontogenetically, this represents a novel mechanism through which fetuses/neonates can raise their platelet counts without increasing platelet production.

The survival of platelets in the circulation is regulated by the balance between anti-apoptotic and pro-apoptotic Bcl-2 family proteins, most notably Bcl-x<sub>L</sub> and Bak.<sup>8,16</sup> Here we found Bcl-x<sub>L</sub> and Bak levels to be similar in neonatal and adult platelets, whereas Bcl-2 was present at significantly higher levels in neonatal platelets, both in mice and humans. The fact that neonatal platelets were also more resistant to apoptosis induced by the Bcl-2/Bcl-x<sub>L</sub> inhibitor ABT-737 suggested that the increased prosurvival signal provided by elevated Bcl-2 levels might allow them to restrain Bak and Bax for an additional day, thereby extending their lifespan in the circulation. However, genetic ablation or pharmacological inhibition of Bcl-2 alone in newborn mice or in human CB-derived platelets did not affect platelet counts and did not shorten neonatal platelet survival or induce apoptosis in vivo or in vitro.

Taken together, our observations suggest that Bcl-2 is functionally redundant in neonatal platelets, and that (despite increased levels) it is not the principal factor that mediates extended neonatal platelet lifespan, nor resistance to ABT-737. It is increasingly clear that the sensitivity or resistance of a given cell to ABT-737 depends on the composition of the complexes formed by prosurvival and proapoptotic proteins in that cell. Indeed, in lymphoid cells, elevated Bcl-2 levels have been shown to confer sensitivity (rather than resistance) to ABT-737.<sup>37</sup> Furthermore, the contribution of BH3-only proteins to the regulation of platelet lifespan is largely unknown, despite evidence that platelet survival is extended in Bad-deficient mice.<sup>38</sup> Although we observed no obvious differences in the expression of the 5 BH3-only proteins examined, it is conceivable that subtle changes in interactions between prosurvival Bcl-x<sub>L</sub> and the BH3-only proteins underpin the changes in platelet lifespan and sensitivity to ABT-737. Alternatively, the resistance to ABT-737 might not be related to the extended neonatal platelet lifespan in vivo. Other as yet unrecognized mechanisms might explain the observed differences.

In conclusion, our findings suggest that neonates might be particularly susceptible to conditions that shorten platelet survival, which may contribute to their high incidence of thrombocytopenia. The current study sets the groundwork for future research aiming at understanding how the neonatal thrombopoietic system responds to changes in platelet production or consumption, and understanding the influence of gestational age on these responses.

## Acknowledgments

The authors thank Dr Maria Ericsson for her technical assistance in electron microscopy and Mr Mark Curry for his technical assistance in MK sorting.

## References

- Castle V, Andrew M, Kelton J, Giron D, Johnston M, Carter C. Frequency and mechanism of neonatal thrombocytopenia. *J Pediatr*. 1986; 108(5 Pt 1):749-755.
- Mehta P, Vasa R, Neumann L, Karpatkin M. Thrombocytopenia in the high-risk infant. *J Pediatr*. 1980;97(5):791-794.
- Christensen RD, Henry E, Wiedmeier SE, et al. Thrombocytopenia among extremely low birth weight neonates: data from a multihospital healthcare system. *J Perinatol*. 2006;26(6): 348-353.
- Liu ZJ, Sola-Visner M. Neonatal and adult megakaryopoiesis. *Curr Opin Hematol*. 2011; 18(5):330-337.
- Klusmann JH, Godinho FJ, Heitmann K, et al. Developmental stage-specific interplay of GATA1 and IGF signaling in fetal megakaryopoiesis and leukemogenesis. *Genes Dev*. 2010;24(15): 1659-1672.
- Mazharian A, Watson SP, Severin S. Critical role for ERK1/2 in bone marrow and fetal liver-derived primary megakaryocyte differentiation, motility, and proplatelet formation. *Exp Hematol*. 2009; 37(10):1238-1249, e1235.
- Bluteau O, Langlois T, Rivera-Munoz P, et al. Developmental changes in human megakaryopoiesis. *J Thromb Haemost*. 2013; 11(9):1730-1741.
- Mason KD, Carpinelli MR, Fletcher JI, et al. Programmed anuclear cell death delimits platelet life span. *Cell*. 2007;128(6):1173-1186.
- Zhang H, Nimmer PM, Tahir SK, et al. Bcl-2 family proteins are essential for platelet survival. *Cell Death Differ*. 2007;14(5):943-951.
- Ren D, Tu HC, Kim H, et al. BID, BIM, and PUMA are essential for activation of the BAX- and BAK-dependent cell death program. *Science*. 2010;330(6009):1390-1393.
- Willis SN, Fletcher JI, Kaufmann T, et al. Apoptosis initiated when BH3 ligands engage multiple Bcl-2 homologs, not Bax or Bak. *Science*. 2007;315(5813):856-859.
- Kodama T, Takehara T, Hikita H, et al. BH3-only activator proteins Bid and Bim are dispensable for Bak/Bax-dependent thrombocyte apoptosis induced by Bcl-xL deficiency: molecular requisites for the mitochondrial pathway to apoptosis in platelets. *J Biol Chem*. 2011;286(16): 13905-13913.
- Schoenwaelder SM, Jarman KE, Gardiner EE, et al. Bcl-xL-inhibitory BH3 mimetics can induce a transient thrombocytopathy that undermines the hemostatic function of platelets. *Blood*. 2011; 118(6):1663-1674.
- Wilson WH, O'Connor OA, Czuczman MS, et al. Navitoclax, a targeted high-affinity inhibitor of BCL-2, in lymphoid malignancies: a phase 1 dose-escalation study of safety, pharmacokinetics, pharmacodynamics, and antitumor activity. *Lancet Oncol*. 2010;11(12):1149-1159.
- Josefsen EC, James C, Henley KJ, et al. Megakaryocytes possess a functional intrinsic apoptosis pathway that must be restrained to survive and produce platelets. *J Exp Med*. 2011; 208(10):2017-2031.
- White MJ, Schoenwaelder SM, Josefsen EC, et al. Caspase-9 mediates the apoptotic death of megakaryocytes and platelets, but is dispensable for their generation and function. *Blood*. 2012; 119(18):4283-4290.
- Hoffmeister KM, Felbinger TW, Falet H, et al. The clearance mechanism of chilled blood platelets. *Cell*. 2003;112(1):87-97.
- Rumjantseva V, Grewal PK, Wandall HH, et al. Dual roles for hepatic lectin receptors in the clearance of chilled platelets. *Nat Med*. 2009; 15(11):1273-1280.
- Kraemer BF, Weyrich AS, Lindemann S. Protein degradation systems in platelets. *Thromb Haemost*. 2013;110(5):920-924.
- Nayak MK, Kulkarni PP, Dash D. Regulatory role of proteasome in determination of platelet life span. *J Biol Chem*. 2013;288(10):6826-6834.
- Hu Z, Slayton WB, Rimsza LM, Bailey M, Sallmon H, Sola-Visner MC. Differences between newborn and adult mice in their response to immune thrombocytopenia. *Neonatology*. 2010;98(1): 100-108.
- Liu ZJ, Italiano J Jr, Ferrer-Marin F, et al. Developmental differences in megakaryocytopoiesis are associated with up-regulated TPO signaling through mTOR and elevated GATA-1 levels in neonatal megakaryocytes. *Blood*. 2011;117(15): 4106-4117.

This work was supported by US National Institutes of Health grants RO1 HL069990 (M.S.-V.), P01 HL046925, HL107146, and HL089224 (K.M.H.), a William Randolph Hearst Foundation Award for Peri- and Prenatal Medicine (Z.-J.L.), a Program Grant (1016647), Fellowship (575506), and an Independent Research Institutes Infrastructure Support Scheme Grant (361646) from the Australian National Health and Medical Research Council, a Fellowship from the Sylvia and Charles Viertel Foundation (B.T.K.), and a Victorian State Government Operational Infrastructure Support Grant. The Sysmex XT-2000i automatic hematology analyzer used in this study was generously provided on an on-loan basis from Sysmex, Kobe, Japan.

## Authorship

Contribution: Z.-J.L. designed and performed experiments, collected and analyzed data, and wrote the manuscript; J.I.Jr. performed and interpreted the electron microscopy studies; Z.H., M.A.D., I.P., E.C.J., H.R., R.G., and C.C. performed experiments; D.E.M., S.A.-O., and P.V.-P. developed and validated the mathematical model; K.M.H. and B.T.K. assisted with experimental design, data interpretation, and preparation of the manuscript; and M.S.-V. supervised and designed experiments, interpreted data, and wrote the manuscript.

Conflict-of-interest disclosure: The authors declare no competing financial interests.

Correspondence: Martha Sola-Visner, Boston Children's Hospital, Division of Newborn Medicine, 300 Longwood Ave, Enders Research Building, Room 961, Boston, MA 02115; e-mail: martha.sola-visner@childrens.harvard.edu; and Zhi-Jian Liu, Boston Children's Hospital, Division of Newborn Medicine, 300 Longwood Ave, Enders Research Building, Room 961, Boston, MA 02115; e-mail: zhi-jian.liu@childrens.harvard.edu.



23. Alugupalli KR, Michelson AD, Barnard MR, Leong JM. Serial determinations of platelet counts in mice by flow cytometry. *Thromb Haemost.* 2001; 86(2):668-671.
24. Sands MS, Barker JE. Percutaneous intravenous injection in neonatal mice. *Lab Anim Sci.* 1999; 49(3):328-330.
25. Mock DM, Mock NI, Lankford GL, Burmeister LF, Strauss RG, Widness JA. Red cell volume can be accurately determined in sheep using a nonradioactive biotin label. *Pediatr Res.* 2008; 64(5):528-532.
26. Berger G, Hartwell DW, Wagner DD. P-Selectin and platelet clearance. *Blood.* 1998;92(11): 4446-4452.
27. Bertino AM, Qi XQ, Li J, Xia Y, Kuter DJ. Apoptotic markers are increased in platelets stored at 37 degrees C. *Transfusion.* 2003;43(7): 857-866.
28. Vogler M, Hamali HA, Sun XM, et al. BCL2/BCL-X (L) inhibition induces apoptosis, disrupts cellular calcium homeostasis, and prevents platelet activation. *Blood.* 2011;117(26):7145-7154.
29. Souers AJ, Levenson JD, Boghaert ER, et al. ABT-199, a potent and selective BCL-2 inhibitor, achieves antitumor activity while sparing platelets. *Nat Med.* 2013;19(2):202-208.
30. Fuertes Marraco SA, Scott CL, Bouillet P, et al. Type I interferon drives dendritic cell apoptosis via multiple BH3-only proteins following activation by PolyI:C in vivo. *PLoS ONE.* 2011;6(6):e20189.
31. Tada T, Widayati DT, Fukuta K. Morphological study of the transition of haematopoietic sites in the developing mouse during the peri-natal period. *Anat Histol Embryol.* 2006;35(4):235-240.
32. Wolber FM, Leonard E, Michael S, Orschell-Traycoff CM, Yoder MC, Srour EF. Roles of spleen and liver in development of the murine hematopoietic system. *Exp Hematol.* 2002;30(9): 1010-1019.
33. Slayton WB, Georgelas A, Pierce LJ, et al. The spleen is a major site of megakaryopoiesis following transplantation of murine hematopoietic stem cells. *Blood.* 2002;100(12):3975-3982.
34. Slayton WB, Wainman DA, Li XM, et al. Developmental differences in megakaryocyte maturation are determined by the microenvironment. *Stem Cells.* 2005;23(9): 1400-1408.
35. Calhoun DA, Li Y, Braylan RC, Christensen RD. Assessment of the contribution of the spleen to granulocytopoiesis and erythropoiesis of the mid-gestation human fetus. *Early Hum Dev.* 1996; 46(3):217-227.
36. Wiedmeier SE, Henry E, Sola-Visner MC, Christensen RD. Platelet reference ranges for neonates, defined using data from over 47,000 patients in a multihospital healthcare system. *J Perinatol.* 2009;29(2):130-136.
37. Mérimo D, Khaw SL, Glaser SP, et al. Bcl-2, Bcl-x(L), and Bcl-w are not equivalent targets of ABT-737 and navitoclax (ABT-263) in lymphoid and leukemic cells. *Blood.* 2012;119(24): 5807-5816.
38. Kelly PN, White MJ, Goschnick MW, et al. Individual and overlapping roles of BH3-only proteins Bim and Bad in apoptosis of lymphocytes and platelets and in suppression of thymic lymphoma development. *Cell Death Differ.* 2010; 17(10):1655-1664.